Fourier Series Solution for Lateral-Torsional Buckling (LTB) of Laterally Braced Beams

Jiangjiang Li[1], Yutong Duan[1], Xiuting Qi[1], Zihan Xing[2], Yucai Zhao[1], Xiaoya Hu[3]
[1]College of Traffic Engineering, Shanxi Vocational University of Engineering Science and Technology, Jinzhong 030619, China
[2]School of Highway, Chang'an University, Xi'an, 710064, China
[3]China Construction Communications Engrg.Group Corp., Ltd., Beijing 100000, China

Corresponding author: Jiangjiang Li (e-mail: lijiangjilin@126.com)

ABSTRACT This study investigates I-beams with discrete lateral bracings subjected to uniform end moments. Initially, the derivation of critical moment formulas is conducted, employing both simple harmonic waves and Fourier series based on trigonometric functions as displacement functions. Subsequently, the impact of the number of terms in the displacement functions on both the LTB strength and threshold stiffness is examined, leading to recommendations for an appropriate number of terms. Ultimately, the calculation formulas are simplified. The findings show that, when the beam is "fully braced" (meaning the brace stiffness is sufficient to allow buckling between the braces of the beam), the derived LTB strength expressions coincide, irrespective of whether a simple harmonic wave or Fourier series is adopted as the displacement function. Divergences in LTB strength formulas emerge solely in scenarios of "partially braced," where the brace is inadequate to permit buckling between braces. The simple harmonic wave form constitutes a special instance within the Fourier series, with the latter's critical moment results offering a refinement over the former's results. The precision of these refined results hinges upon the number of terms in the Fourier series, with the optimal number intimately tied to the number of braces. Consequently, this study advocates that in deriving the LTB strength of laterally braced beams via the energy method, the selection of terms in the displacement function ought to be $2 \times$ (the number of brace +1).

INDEX TERMS I-beam with discrete lateral bracings; lateral-torsional buckling; energy method; fourier series; displacement functions

Notation

a_L	the vertical distance between the point bracing and the shear centre of the cross-section, $\widetilde{a}_L$ is the dimensionless coefficient of a_L	$M_{0,i}$	critical moment without braces to i buckling half-wave
a_b	sectional parameters	$M_{cr,(n_b+1)}$	critical moment for fully braced structure, $\widetilde{M}_{cr,(n_b+1)}$ is the dimensionless coefficient
β_L	lateral brace stiffness, $\widetilde{\beta}_L$ is the dimensionless coefficient of β_L	m	the m-th bracing along the positive OZ direction
β_y	cross-sectional asymmetry parameter, $\widetilde{\beta}_y$ is the dimensionless coefficient of β_y	h_0	height of I-beam
E	Yang's modulus	n_0	the determination of the number of terms
G	shear modulus	n_b	number of lateral bracings
i	number of half-wave of buckling	N	the total number of effective terms affecting the waveform in the first n_0 terms
I_t	pure torsional constant	t_w	web thickness
I_ω	warping constant	t_f	flange thickness
I_y	moment of inertia about the weak axis of the section	u	lateral displacement of the section
I_{yc}	moment of inertia of the compressed flange about the weak axis	$u(z)$	deformation function for lateral displacement at the shear centre
κ	torsional slenderness	θ	twist angle of the section
L	length of I-beam	$\theta(z)$	deformation function for sectional twist angle
L_b	distance between bracings	Π_b	the potential energy contributed by the lateral bracing
M_x	bending moment about the strong axis of the section	Π_{pur}	total potential energy
$M_{cr,i}$	critical moment for partially braced structure to i buckling half-wave, $\widetilde{M}_{cr,i}$ is the dimensionless coefficient		

I. INTRODUCTION

THE bracing for beams can be categorized as lateral bracing and torsional bracing [1]. Beams with such bracing are respectively referred to as laterally braced beams and torsionally braced beams. The relevant provisions outlined in the AISC-360 [2] specification for beam bracing are largely based on Yura's research. Nonetheless, in scenarios where Yura's findings are applied to beams featuring discrete lateral bracings, it becomes imperative to equate the stiffness of these discrete bracings to a continuous stiffness spanning the entire length of the beam. Some scholars [3] argued that this equivalence of stiffness to a continuous form may not always be precise. Consequently, it is necessary to start directly from the discrete lateral stiffness and use static or energy methods to determine the LTB strength.

The static method necessitates the resolution of differential equations to derive the closed-form solution for the LTB strength. In scenarios where the number of braces is substantial, the derivation of such a closed-form solution via the static method becomes exceedingly complex. Alternatively, the Rayleigh-Ritz method (energy method) offers a pathway to determining an approximate solution for the LTB strength. Based on the principle of stationary potential energy, this method involves the selection of a displacement function that adhere to geometric constraints. It then seeks the variational extremum under conditions where the structure's total potential energy remains invariant, essentially solving for the displacement state that corresponds to a stationary total potential energy. The precision of the analysis when employing the Rayleigh-Ritz method hinges on the accuracy of the chosen displacement functions [4]. To ascertain the LTB strength of beam with lateral bracing, it is imperative to identify suitable displacement functions for both the lateral displacement $u(z)$ at the shear center and the sectional rotation $\theta(z)$. These displacement functions must not only satisfy the geometric boundary conditions but also closely align with the actual deformation characteristics of the beam [5, 6].

Using the simply supported beam as an illustrative case, the boundary conditions imposed by its "fork support" necessitate that the end lateral displacement remain nil, while the ends must remain untwisted yet free to warp, i.e. $u(0) = u(L) = 0$, $\theta(0) = \theta(L) = 0$, and $\theta''(0) = \theta''(L) = 0$. For beams without bracing, the first buckling mode exhibits a sinusoidal half-wave pattern, thus allowing the utilization of a single sine function (also termed as a simple harmonic function) to represent the displacement functions, namely $u(z) = u_1 \sin(\pi z/L)$ and $\theta(z) = \theta_1 \sin(\pi z/L)$. For beams with lateral bracing, where the number of braces is denoted as n_b, the buckling wave number i can span from 1 to n_b+1, depending on the brace stiffness.

A minimum of n_b+1 terms in the displacement function, specifically $u(z) = \sum_{n=1}^{n_b+1} u_n \sin(n\pi z/L)$ and $\theta(z) = \sum_{n=1}^{n_b+1} \theta_n \sin(n\pi z/L)$, are required to ascertain all the relevant modes. Nevertheless, when the number of terms is n_b+1, the displacement function essentially aligns with the simple harmonic function characteristic of an unbraced beam. Specifically, the function $u(z) = u_2 \sin(2\pi z/L)$ is solely capable of determining the LTB strength corresponding to a buckling wave number of 2, while $u(z) = u_{n_b} \sin(n_b\pi z/L)$ is exclusively associated with determining the LTB strength at a buckling wave number of n_b, both being independent of any other terms. To elucidate further, when the number of brace is n_b and the displacement function comprises n_b+1 terms, each buckling wave number i corresponds to a distinct sine function. This scenario is defined as one where the effective function influencing the waveform consists of a single term, and the displacement function $u(z) = \sum_{n=1}^{n_b+1} u_n \sin(n\pi z/L)$ is also characterized as the simple harmonic wave form for beam with n_b braces. Nonetheless, owing to the discontinuous nature of the lateral bracing and the variability in stiffness, the beam's deformation during buckling grows more intricate, potentially deviating from a perfect simple harmonic wave form. If the number of terms is fixed at n_b+1, it may lead to significant errors, with the magnitude of these errors increasing as the number of braces rises.

Given that the Fourier series is infinite, it can represent any displacement curve, leading to its widespread application in the displacement functions of beams [7-10]. In cases where the displacement functions of braced beams are expressed using the Fourier series, denoted as $u(z) = \sum_{n=1}^{\infty} u_n \sin(n\pi z/L)$ and $\theta(z) = \sum_{n=1}^{\infty} \theta_n \sin(n\pi z/L)$, all derivatives of these displacement functions can be directly obtained through term-by-term differentiation of their Fourier series representations. As the number of terms increases, the more effective functions contribute to the buckling waveform, resulting in a fitted curve that closely aligns with the actual displacement curve, thereby producing results that closely approximate true values. However, this comes at the cost of exponentially increasing computational complexity [11]. Consequently, when considering only the first n_0 terms of the Fourier series for the displacement functions, denoted as $u(z) = \sum_{n=1}^{n_0} u_n \sin(n\pi z/L)$ and $u(z) = \sum_{n=1}^{n_0} u_n \sin(n\pi z/L)$, it becomes crucial to determine an appropriate value of n_0 that balances computational simplicity with sufficient accuracy.

This paper takes I-beams with discrete lateral bracing under equal end moments as the research object. Initially, the formulas for LTB strength are derived by employing simple harmonic wave and Fourier series as displacement functions. Building upon the Fourier series analysis, the impact of the number of terms within the displacement function on both the LTB strength and the threshold stiffness is then examined. Ultimately, judicious recommendations for the appropriate number of function terms are provided, and the computational formula is streamlined.

II. COMPARISON OF SIMPLE HARMONIC WAVES AND FOURIER SERIES FOR LTB STRENGTH CALCULATION

A. POTENTIAL ENERGY EQUATION

As shown in Figure 1, the coordinate system OXYZ is established, where O represents the centroid of the cross-section, OY is along the beam's height direction, and OZ is along the beam's length direction. For a simply supported beam with a span of L that is subjected to equal end moment M_x, assuming that n_b point bracings are evenly spaced along the length of the beam, and these braces are labeled along the Z-axis as Z_m (the subscript m denotes the m-th bracing along the positive OZ direction, $m \in [1, n_b]$), where the distance between bracings is $L_b = L/(n_b+1)$. Thus, under the action of equal end moments, the total potential energy equation [12-16] for the beam is represented by Eq. (1).

$$\Pi = \frac{1}{2}\int_0^L \big(EI_y u''^2 + EI_\omega \theta''^2 + GI_t \theta'^2 + 2M_x\beta_y\theta'^2 + 2M_x u''\theta\big)\, dz + \sum_{m=1}^{n_b} \frac{1}{2}\beta_L u_m^2. \tag{1}$$

Where E is the Yang's modulus, G is the shear modulus, I_y is the moment of inertia about the weak axis of the cross-section, I_ω is the sectorial moment of inertia or warping constant, I_t is the pure torsional constant, and β_y is the cross-sectional asymmetry parameter [17]. The quantities u and θ represent the lateral displacement and twist angle of the cross-section; u' and θ' are the first derivatives of u and θ, and u'' and θ'' are the second derivatives of u and θ. The parameter β_L represents the brace stiffness; $u_m = u + a_L\theta$ represents the lateral displacement at the m-th brace, and a_L represents the vertical distance between the point bracing and the shear center "C" of the cross-section. A positive value signifies that the bracing is positioned on the side of the shear center which is proximate to the compression flange, whereas a negative value denotes its location on the side nearer to the tension flange, as illustrated in Figure 2. $\tilde{a}_L = a_L/(h_0/2)$, where $\tilde{a}_L$ is the dimensionless coefficient of a_L and h_0 represents the height of the beam.

B. SIMPLE HARMONIC WAVE

Based on previous research on lateral braced column [18], it is evident that the buckling mode of these columns can exhibit varying buckling waveforms, influenced by the brace stiffness. In the context of a structure under "fully braced," buckling occurs between adjacent braces. The minimal stiffness necessary to satisfy such conditions is termed the threshold stiffness. If the brace stiffness exceeds this threshold, the number of buckling waves becomes exclusively dependent on the number of braces. Conversely,

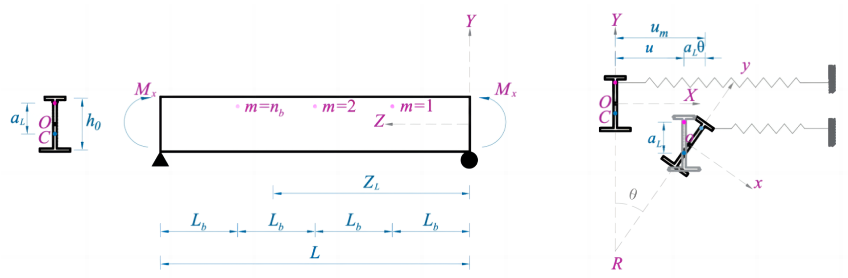

FIGURE 1. I-beam with lateral bracings

when the brace stiffness falls below the threshold—a state also known as "partially braced"—the number of buckling waves is predominantly influenced by the brace stiffness. These concept systems remain valid and applicable when examining beams.

Supposing that the displacement function takes the form of Eq. (2), wherein u_n and θ_n represent the amplitudes of the trigonometric displacement.

$$u(z)=\sum_{n=1}^{n_b+1}u_n\sin\left(\frac{n\pi z}{L}\right),\quad \theta(z)=\sum_{n=1}^{n_b+1}\theta_n\sin\left(\frac{n\pi z}{L}\right). \tag{2}$$

When the buckling wave number i is equivalent to n_b+1, the structural buckling waveform comprises n_b+1 identical sine half-waves. In this state, the structure attains "fully braced," and consequently, the potential energy increment resulting from the lateral bracing is nil. The critical bending moment for the laterally braced beam is given by Eq. (3) and the non-dimensional critical bending moment are is provided in Eqs. (4) to (5).

$$\begin{aligned}M_{cr,(n_b+1)}=&\frac{\pi^2EI_y}{L^2/(n_b+1)^2}\cdot\frac{h_0}{2}\\&\times\left[\widetilde{\beta}_y+\sqrt{\widetilde{\beta}_y^2+4\alpha_b(1-\alpha_b)\left(1+\frac{\kappa^2}{(n_b+1)^2}\right)}\right].\end{aligned} \tag{3}$$

$$\widetilde{M}_{cr,(n_b+1)}=M_{cr,(n_b+1)}\bigg/\left(\frac{\pi^2EI_y}{L^2}\cdot\frac{h_0}{2}\right). \tag{4}$$

$$\begin{aligned}\widetilde{M}_{cr,(n_b+1)}=&(n_b+1)^2\widetilde{\beta}_y\\&+\sqrt{\begin{aligned}&(n_b+1)^4\widetilde{\beta}_y^2\\&+4\alpha_b(1-\alpha_b)\left[(n_b+1)^4+(n_b+1)^2\kappa^2\right]\end{aligned}}\end{aligned} \tag{5}$$

In the equation, $\widetilde{\beta}_y$, κ, and α_b are sectional parameters, where $\widetilde{\beta}_y=\beta_y/(h_0/2)$, $\kappa^2=GI_tL^2/(\pi^2EI_\omega)$, and $\alpha_b=I_{yc}/I_y$; I_{yc} is the moment of inertia of the compression flange about the weak axis. In addition, $\widetilde{\beta}_T=\beta_T/(\pi^2EI_\omega/L_b^3)$, where $\widetilde{\beta}_T$ is the dimensionless coefficient of β_T, also known as the dimensionless brace stiffness.

When the buckling wave number $i\in[1,n_b]$, the structure is in a state of "partially braced". The potential energy contributed by the lateral bracing is as shown in Eq. (6). As a result, the total potential energy equation for the beam is presented in Eq. (7), with all symbols previously defined in the text.

$$\Pi_b=\frac{n_b+1}{4}\beta_L\left(u_n+a_L\theta_n\right)^2. \tag{6}$$

$$\begin{aligned}\Pi_{pur}=&\frac{EI_yn^4\pi^4}{4L^3}u_n^2+\frac{EI_\omega n^4\pi^4}{4L^3}\theta_n^2\\&+\left(\frac{GI_tn^2\pi^2}{4L}+\frac{M_x\beta_yn^2\pi^2}{2L}\right)\theta_n^2\\&-\frac{M_xn^2\pi^2}{2L}u_n\theta_n+\frac{n_b+1}{4}\beta_L\left(u_n+a_L\theta_n\right)^2.\end{aligned} \tag{7}$$

By setting $\partial\Pi_{pur}/\partial u_n=0$ and $\partial\Pi_{pur}/\partial\theta_n=0$, the expressions for the non-dimensional critical moment associated with various buckling wave numbers i are derived, as presented in Eqs. (8)–(9).

$$\widetilde{M}_{cr,i}=M_{cr,i}\bigg/\left(\frac{\pi^2EI_y}{L^2}\cdot\frac{h_0}{2}\right). \tag{8}$$

$$\begin{aligned}\widetilde{M}_{cr,i}=&i^2\widetilde{\beta}_y+\left(\widetilde{\beta}_y+\widetilde{a}_L\right)\frac{\widetilde{\beta}_0}{i^2}\\&+\sqrt{\begin{aligned}&\left(i^2+\frac{\widetilde{\beta}_0}{i^2}\right)\left[i^2\widetilde{\beta}_y^2+\left(\widetilde{\beta}_y+\widetilde{a}_L\right)^2\frac{\widetilde{\beta}_0}{i^2}\right.\\&\left.\qquad+4\alpha_b(1-\alpha_b)(i^2+\kappa^2)\right]\end{aligned}}.\end{aligned} \tag{9}$$

$$\widetilde{\beta}_0=\frac{(n_b+1)^4}{\pi^2}\widetilde{\beta}_L=\frac{(n_b+1)\beta_LL_b^3}{\pi^4EI_y}. \tag{10}$$

To conclude, the equation for determining the non-dimensional critical moment of laterally braced beam is presented in Eq. (11).

$$\widetilde{M}_{cr}=\min\left\{\widetilde{M}_{cr,i},\widetilde{M}_{cr,(n_b+1)}\right\},\quad i\in[1,n_b]. \tag{11}$$

C. FOURIER SERIES

The displacement function of the beam is assumed to take the form of a Fourier series, as depicted in Eq. (12).

$$u(z)=\sum_{n=1}^{\infty}u_n\sin\left(\frac{n\pi z}{L}\right),\quad \theta(z)=\sum_{n=1}^{\infty}\theta_n\sin\left(\frac{n\pi z}{L}\right). \tag{12}$$

By the same token, it can be derived that Critical moment for fully braced structure:

$$\widetilde{M}_{cr,(n_b+1)} = (n_b+1)^2\widetilde{\beta}_y + \sqrt{\begin{aligned}&(n_b+1)^4\widetilde{\beta}_y^2\\ &+4\alpha_b(1-\alpha_b)\left[(n_b+1)^4+(n_b+1)^2\kappa^2\right]\end{aligned}} \tag{13}$$

$$M_{cr,(n_b+1)} = \left(\frac{\pi^2 EI_y}{L^2}\frac{h_0}{2}\right)\widetilde{M}_{cr,(n_b+1)}. \tag{14}$$

Critical moment for partially braced structure:

$$1+\frac{(n_b+1)^4}{\pi^2}\widetilde{\beta}_L\sum_{j=1}^{\infty}\eta_{n_{ij}}=0, \quad i\in[1,n_b]. \tag{15}$$

$$\eta_{n_{ij}} = \frac{\begin{aligned}&4\alpha_b(1-\alpha_b)(n_{ij}^2+\kappa^2)+2\widetilde{a}_L\widetilde{M}_{cr,i}\\ &+2\widetilde{\beta}_y\widetilde{M}_{cr,i}+n_{ij}^2\widetilde{a}_L^2\end{aligned}}{\begin{aligned}&4\alpha_b(1-\alpha_b)n_{ij}^2(n_{ij}^4+n_{ij}^2\kappa^2)\\ &+n_{ij}^2\left(2n_{ij}^2\widetilde{\beta}_y\widetilde{M}_{cr,i}-\widetilde{M}_{cr,i}^2\right)\end{aligned}} \tag{16}$$

$$n_{ij} = \begin{cases} i, & j=1,\\ j(n_b+1)-i, & j=2,4,6,\ldots,\\ (j-1)(n_b+1)+i, & j=3,5,7,\ldots. \end{cases} \tag{17}$$

$$M_{cr,i} = \left(\frac{\pi^2 EI_y}{L^2}\cdot\frac{h_0}{2}\right)\widetilde{M}_{cr,i}. \tag{18}$$

When the brace stiffness is zero, the Critical moment is:

$$\widetilde{M}_{0,i} = i^2\widetilde{\beta}_y + \sqrt{i^4\widetilde{\beta}_y^2+4\alpha_b(1-\alpha_b)\left(i^4+i^2\kappa^2\right)}. \tag{19}$$

$$M_{0,i} = \left(\frac{\pi^2 EI_y}{L^2}\cdot\frac{h_0}{2}\right)\widetilde{M}_{0,i}. \tag{20}$$

$$\widetilde{M}_{0,i} \le \widetilde{M}_{cr,i} \le \widetilde{M}_{cr,(n_b+1)}. \tag{21}$$

III. THE INFLUENCE OF THE NUMBER OF TERMS IN THE DISPLACEMENT FUNCTION

It has been observed that the critical moment expressions for conditions of "full braced" are identical when derived using either the simple harmonic wave or the Fourier series as the displacement function. Divergence in the critical moment calculations by these two methods occurs only under "partially braced" conditions, where the Fourier series form proves to be more rational for computation. Nonetheless, employing the Fourier series form, which entails taking an infinite number of terms in the displacement function as depicted in Eq. (12), is intrinsically complex and thus necessitates simplification. A simplified displacement function is postulated, as depicted in Eq. (22), and the focus shifts to determining an appropriate value for n_0 that ensures the critical moment formula derived from this simplified displacement function meets the requisite accuracy standards.

$$u(z)=\sum_{n=1}^{n_0}u_n\sin\left(\frac{n\pi z}{L}\right), \quad \theta(z)=\sum_{n=1}^{n_0}\theta_n\sin\left(\frac{n\pi z}{L}\right). \tag{22}$$

The computation of $\widetilde{M}_{cr,i}$ is contingent upon the parameters n_b, α_b, $\widetilde{\beta}_y$, κ, $\widetilde{a}_L$, and $\eta_{n_{ij}}$. Among the various parameters, only $\eta_{n_{ij}}$ bears relevance to the determination of the number of terms n_0. Consequently, a thorough examination of $\eta_{n_{ij}}$ is prerequisite to attaining the objective of simplification. Within the coefficient $\eta_{n_{ij}}$, the subscript i signifies the number of buckling waves, whereas j denotes the j-th effective term in the Fourier series. An effective term, in this context, is one that influences the waveform; for a simple harmonic wave, this is represented by the numeral 1. Assuming that the total number of effective terms affecting the waveform in the first n_0 terms is N, $j\in[1,N]$. Hence, the physical significance of $\eta_{n_{ij}}$ lies in its representation of the j-th effective term, given that the count of buckling waves is i.

To elucidate the physical significance of $\eta_{n_{ij}}$, an illustrative example is presented. Suppose the number of braces is $n_b=2$, and the buckling wave number i ranges from 1 to 3, depending on the brace stiffness. Consequently, Eq. (17) yields $n_{11}=1$, $n_{21}=2$, $n_{31}=3$, $n_{12}=5$, $n_{22}=4$, $n_{32}=3$, $n_{13}=7$, $n_{23}=8$, and $n_{33}=9$. When the number of terms n_0 is taken as 6, $n_{13}=7$, $n_{23}=8$, and $n_{33}=9$ are invalid due to the condition $n_{ij}\le n_0$. Hence, It can be obtained that $N=2$ and $j\in[1,2]$. This implies that the displacement function is composed of two effective sine functions. Subsequently, an elaboration on these two valid sine functions will be provided individually. Specifically, the values $n_{11}=1$, $n_{21}=2$, and $n_{31}=3$ represent the respective initial effective terms corresponding to buckling wave numbers of 1, 2, and 3. Thus, the respective valid functions are denoted as $u(z)=u_1\sin(\pi z/L)$, $u(z)=u_2\sin(2\pi z/L)$, and $u(z)=u_3\sin(3\pi z/L)$. Similarly, $n_{12}=5$, $n_{22}=4$, and $n_{32}=3$ signify the secondary effective terms associated with buckling wave numbers of 1, 2, and 3, corresponding to $u(z)=u_5\sin(5\pi z/L)$, $u(z)=u_4\sin(4\pi z/L)$, and $u(z)=u_3\sin(3\pi z/L)$, respectively. In summary, when $n_b=2$ and $n_0=6$, the displacement function's effective component for the structure exhibiting one buckling wave is denoted as $u(z)=u_1\sin(\pi z/L)+u_5\sin(5\pi z/L)$. This implies that the superposition of the two trigonometric functions influences a single buckling wave. Similarly, for the structure manifesting two buckling waves, the effective displacement function is represented by $u(z)=u_2\sin(2\pi z/L)+u_4\sin(4\pi z/L)$, and for three buckling waves, it is $u(z)=u_3\sin(3\pi z/L)$.

To further elucidate the distinction between Fourier series analysis and simple harmonic wave analysis, a hypothetical scenario is considered wherein $n_b=2$ and $n_0=6$. It can be found that $n_{11}=1$, $n_{21}=2$, $n_{31}=3$, and $n_{32}=3$ are effective. That is, the displacement function $u(z)=u_1\sin(\pi z/L)$ corresponds to the structure exhibiting one buckling wave, $u(z) = u_2 \sin(2\pi z/L)$ to two buckling waves, and $u(z) = u_3 \sin(3\pi z/L)$ to three buckling waves. Notably, in this context, the displacement functions align with those derived from simple harmonic wave analysis.

Therefore, it can be concluded that the effective sine functions vary depending on the number of terms n_0, when the structure exhibits i buckling waves. Notably, when the condition $n_0 = n_b + 1$ is met, the analysis outcomes derived from the Fourier series as the displacement function can be simplified to align with those of the simple harmonic wave as the displacement function. Based on Eq. (17), it is evident that when $N = 1$, the range of n_0 is $i \le n_0 < 2(n_b+1)-i$; similarly, when $N = 2$, $2(n_b+1)-i \le n_0 < 2(n_b+1)+i$; and when $N = 3$, $2(n_b+1)+i \le n_0 < 4(n_b+1)-i$. This pattern continues, and the relationship between N and n_0 can be deduced in Eq. (23).

$$\begin{cases} N = 1,3,5,7,\ldots, \\ \qquad (N-1)(n_b+1)+i \le n_0 < (N+1)(n_b+1)-i, \\ N = 2,4,6,8,\ldots, \\ \qquad N(n_b+1)-i \le n_0 < N(n_b+1)+i, \end{cases}$$
$$i \in [1, n_b]. \tag{23}$$

It is evident that the range of term number varies with differing i for a given N. Specifically, when $N = 1$, it can be observed that $1 \le n_0 < 2n_b + 1$ if $i = 1$; $2 \le n_0 < 2n_b$ if $i = 1$; $n_b - 1 \le n_0 < n_b + 3$ if $i = n_b - 1$; and $n_b \le n_0 < n_b + 2$ if $i = n_b$. Table 1 outlines the corresponding N values for various i and term number n_0, where "—" signifies that the value does not exist.

Based on the aforementioned analysis, it is evident that variations in the term number n_0, given a known number of buckling waves i, can result in differing N values and $\widetilde{M}_{cr,i}$. Taking into account the influence of the term number n_0 of the displacement function, Eq. (15) can be converted to Eq. (24).

$$1 + \frac{(n_b+1)^4}{\pi^2}\widetilde{\beta}_L \sum_{j=1}^{N} \eta_{n_{ij}} = 0, \quad i \in [1, n_b]. \tag{24}$$

To differentiate the $\widetilde{M}_{cr,i}$ computed for varying numbers of effective functions N, it is denoted as $\widetilde{M}_{(cr,i)-N}$. Specifically, when $N = 1$, indicating that n_{ij} comprises a single element n_{i1}, $\widetilde{M}_{cr,i}$ is derived using the formula $1 + \widetilde{\beta}_0 \eta_{n_{i1}} = 0$ and is labeled as $\widetilde{M}_{(cr,i)-1}$. In the case where $N = 2$, signifying that n_{ij} consists of two elements, n_{i1} and n_{i2}, $\widetilde{M}_{cr,i}$ is determined by the formula $1 + \widetilde{\beta}_0(\eta_{n_{i1}} + \eta_{n_{i2}}) = 0$ and is designated as $\widetilde{M}_{(cr,i)-2}$. To generalize, for any given number of values N, the $\widetilde{M}_{cr,i}$ calculated according to Eq. (24) is designated as $\widetilde{M}_{(cr,i)-N}$, where N is contingent upon the term number n_0 in the displacement function.

Hence, under the specified conditions, the non-dimensional critical moment $\widetilde{M}_{cr}$ is dictated by the term number n_0 in the displacement function. Specifically, when $n_0 = n_b + 1$, the calculation formula for $\widetilde{M}_{cr}$ is presented in Eq. (25). In the case where $n_0 = n_b + 2$, the formula is given by Eq. (26), with the distinction between Eqs. (26) and (25) being attributed to the differences between $\widetilde{M}_{(cr,n_b)-2}$ and $\widetilde{M}_{(cr,n_b)-1}$. Here, $\widetilde{M}_{(cr,n_b)-2}$ serves as a correction to $\widetilde{M}_{(cr,n_b)-1}$, stemming from the augmented number of terms. Furthermore, when $n_0 = 2n_b$, $\widetilde{M}_{cr}$ is calculated using Eq. (27), wherein $\widetilde{M}_{(cr,i)-2}$ is interpreted as a correction to $\widetilde{M}_{(cr,i)-1}$. Analogously, $\widetilde{M}_{(cr,n_b)-N}$ is viewed as a correction to $\widetilde{M}_{(cr,i)-1}$ after accounting for the term number n_0. To illustrate, consider a laterally braced beam with $n_b = 2$ and $\kappa^2 = 0.5$; Figure 2 depicts a comparison of $\widetilde{M}_{(cr,i)-N}$ for different number of terms n_0. Notably, when $N \ge 2$, the computed results exhibit minimal variation.

When $n_0 = n_b + 1$,

$$\begin{aligned} \widetilde{M}_{cr} = \min\{&\widetilde{M}_{(cr,1)-1}, \widetilde{M}_{(cr,2)-1}, \widetilde{M}_{(cr,3)-1}, \ldots, \\ &\widetilde{M}_{(cr,n_b)-1}, \widetilde{M}_{cr,(n_b+1)}\}. \end{aligned} \tag{25}$$

When $n_0 = n_b + 2$,

$$\begin{aligned} \widetilde{M}_{cr} = \min\{&\widetilde{M}_{(cr,1)-1}, \widetilde{M}_{(cr,2)-1}, \widetilde{M}_{(cr,3)-1}, \ldots, \\ &\widetilde{M}_{(cr,n_b)-2}, \widetilde{M}_{cr,(n_b+1)}\}. \end{aligned} \tag{26}$$

When $n_0 = 2n_b$,

$$\begin{aligned} \widetilde{M}_{cr} = \min\{&\widetilde{M}_{(cr,1)-1}, \widetilde{M}_{(cr,2)-2}, \widetilde{M}_{(cr,3)-2}, \ldots, \\ &\widetilde{M}_{(cr,n_b)-2}, \widetilde{M}_{cr,(n_b+1)}\}. \end{aligned} \tag{27}$$

When $n_0 = 2(n_b + 1)$,

$$\begin{aligned} \widetilde{M}_{cr} = \min\{&\widetilde{M}_{(cr,1)-2}, \widetilde{M}_{(cr,2)-2}, \widetilde{M}_{(cr,3)-2}, \ldots, \\ &\widetilde{M}_{(cr,n_b)-2}, \widetilde{M}_{cr,(n_b+1)}\}. \end{aligned} \tag{28}$$

IV. ANALYSIS OF THE APPROPRIATE NUMBER OF TERMS FOR THE DISPLACEMENT FUNCTION

As previously stated, when $N > 1$, $\widetilde{M}_{(cr,i)-N}$ is determined through the equation $1 + \widetilde{\beta}_0(\eta_{n_{i1}} + \eta_{n_{i2}} + \cdots + \eta_{n_{ij}}) = 0$. Given the assumption of the relationship $|\eta_{n_{i1}}| \gg |\eta_{n_{ij}}|$, the coefficient $\eta_{n_{ij}}$ becomes negligible. The symbol χ_j, defined in Eq. (29), signifies the absolute value of the ratio between coefficients $\eta_{n_{i1}}$ and $\eta_{n_{ij}}$. Specifically, $\chi_2 = |\eta_{n_{i1}}/\eta_{n_{i2}}|$ denotes the absolute value of the ratio of $\eta_{n_{i1}}$ to $\eta_{n_{i2}}$. Consequently, it is imperative to ascertain the χ_j values corresponding to various i values, enabling the omission of smaller $\eta_{n_{ij}}$ and thereby facilitating simplification.

$$\chi_j = \left|\frac{\eta_{n_{i1}}}{\eta_{n_{ij}}}\right|. \tag{29}$$

The value of χ_j is influenced not only by section parameters and brace conditions but also by the buckling wave number i. Using a double-symmetric beam characterized by $\widetilde{a}_L \in (0,1)$, $\kappa^2 \in (0,50)$, and $n_b \in (0,10)$ (where $\widetilde{a}_L \ge 0$ signifies that the brace is positioned above the shear center) as an illustrative case, the relationship between χ_j and i

TABLE 1. Values of N for various i and term number n_0

i/n_0	1	2	$\cdots$	n_b-1	n_b	n_b+1	$(n_b+1)+1$	$\cdots$	$(n_b+1)+n_b$	$2(n_b+1)$
$i=1$	$N=1$	$N=1$	$\cdots$	$N=1$	$N=1$	$N=1$	$N=2$	$\cdots$	$N=2$	$\cdots$
$i=2$	–	$N=1$	$\cdots$	$N=1$	$N=1$	$N=1$	$N=1$	$\cdots$	$N=2$	$N=2$
$i=3$	–	–	$\cdots$	$N=1$	$N=1$	$N=1$	$N=2$	$\cdots$	$N=2$	$N=2$
$\vdots$	$\vdots$	$\vdots$	$\ddots$	$\vdots$	$\vdots$	$\vdots$	$\vdots$	$\ddots$	$\vdots$	$\vdots$
$i=n_b-2$	–	–	$\cdots$	$N=1$	$N=1$	$N=1$	$N=1$	$\cdots$	$N=2$	$N=2$
$i=n_b-1$	–	–	$\cdots$	$N=1$	$N=1$	$N=1$	$N=2$	$\cdots$	$N=2$	$N=2$
$i=n_b$	–	–	$\cdots$	–	$N=1$	$N=1$	$N=2$	$\cdots$	$N=2$	$N=2$

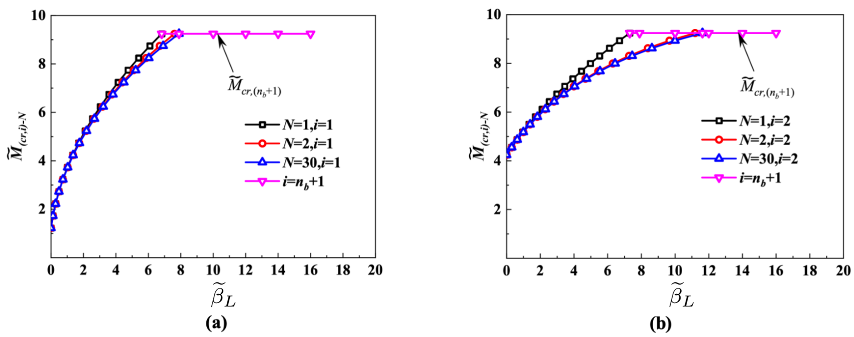

FIGURE 2. Comparison of $\widetilde{M}_{(cr,i)-N}$ for different number of terms n_0: (a) $i=1$; (b) $i=2$

is elucidated. As depicted in Figure 3, for $n_b = 10$, the specific values of χ_2 and χ_3 are presented. Notably, when $i = 1$, χ_2 reaches a minimum of 12.3 and χ_3 reaches a minimum of 18.1, suggesting that $|\eta_{n_{i1}}|$ is at least 12.3 times greater than $|\eta_{n_{i2}}|$ and at least 18.1 times greater than $|\eta_{n_{i3}}|$. Similarly, when $i = n_b$, the minimum values for χ_2 and χ_3 are 1.31 and 222.8, respectively. Consequently, within the interval $(1, n_b)$ for i, it follows that $\chi_2 \in (1.31, 12.3)$ and $\chi_3 \in (18.1, 222.8)$.

When varying the number of braces n_b, the minimum values of χ_j are presented in Tables 2 and 3. Notably, when $i \to 1$, $|\eta_{n_{i1}}|$ exceeds $|\eta_{n_{i2}}|$ by a factor of over 10; when $i \to n_b$, the values of $|\eta_{n_{i1}}|$ and $|\eta_{n_{i2}}|$ are comparable, and $|\eta_{n_{i1}}|$ surpasses $|\eta_{n_{i3}}|$ by a factor exceeding 40. In the equation $1+\widetilde{\beta}_0(\eta_{n_{i1}}+\eta_{n_{i2}}+\cdots+\eta_{n_{ij}}) = 0$, retaining only $\eta_{n_{i1}}$ and $\eta_{n_{i2}}$ suffices to attain simplification.

TABLE 2. The calculation result for $i = 1$

χ_j / n_b	$\lvert\eta_{n_{i1}}/\eta_{n_{i2}}\rvert$	$\lvert\eta_{n_{i1}}/\eta_{n_{i3}}\rvert$	$\lvert\eta_{n_{i1}}/\eta_{n_{i4}}\rvert$	$\lvert\eta_{n_{i1}}/\eta_{n_{i5}}\rvert$	$\lvert\eta_{n_{i1}}/\eta_{n_{i6}}\rvert$	$\lvert\eta_{n_{i1}}/\eta_{n_{i7}}\rvert$
1	4.33	40.6	159.0	436.3	975.0	1903.0
2	6.80	29.0	182.0	356.0	1043	1628.0
3	8.41	24.7	197.5	326.5	1096.4	1530.8
4	9.51	22.4	207.8	310.6	1132.5	1479.0
5	10.3	21.0	215.1	300.6	1157.8	1446.2
6	10.9	20.1	220.4	293.7	1176.4	1423.5
7	11.4	19.4	224.5	288.6	1190.6	1406.7
8	11.7	18.9	227.7	284.7	1201.8	1393.9
9	12.0	18.4	230.4	281.6	1210.8	1383.7
10	12.3	18.1	232.5	279.1	1218.3	1375.4

TABLE 3. The calculation result for $i = 1$

χ_j / n_b	$\lvert\eta_{n_{i1}}/\eta_{n_{i2}}\rvert$	$\lvert\eta_{n_{i1}}/\eta_{n_{i3}}\rvert$	$\lvert\eta_{n_{i1}}/\eta_{n_{i4}}\rvert$	$\lvert\eta_{n_{i1}}/\eta_{n_{i5}}\rvert$	$\lvert\eta_{n_{i1}}/\eta_{n_{i6}}\rvert$	$\lvert\eta_{n_{i1}}/\eta_{n_{i7}}\rvert$
1	4.33	40.6	159.0	436.3	975.0	1903.0
2	2.69	61.8	152.2	589.7	1007.0	2460.3
3	2.11	82.2	161.7	743.2	1109.8	3035.3
4	1.82	102.4	175.9	897.4	1236.7	3619.8
5	1.65	122.5	192.2	1052.1	1374.4	4209.3
6	1.53	142.6	209.8	1207.1	1517.8	4801.8
7	1.45	162.3	228.0	1362.4	1664.7	5396.2
8	1.39	182.7	246.7	1517.8	1813.7	5991.8
9	1.35	202.7	265.6	1673.4	1964.3	6588.3
10	1.31	222.8	284.8	1829.0	2115.9	7185.4

V. VALIDATION AND COMPARATIVE ANALYSIS OF SIMPLIFIED EQUATIONS

A. *SIMPLIFIED EQUATIONS*

Based on the aforementioned analysis, it is evident that setting $N = 2$ during the simplification process suffices to meet the required computational accuracy. In this scenario, the number of terms in the displacement function equates to $n_0 = 2(n_b+1)$, allowing Eq. (24) to be simplified to Eq. (30). Naturally, when the number of terms $n_0 > 2(n_b+1)$, the computational outcomes are more accurate, but the computational difficulty is greater.

$$1+\frac{(n_b+1)^4}{\pi^2}\widetilde{\beta}_L\left(\eta_{n_{i1}}+\eta_{n_{i2}}\right)=0, \quad i\in[1,n_b]. \tag{30}$$

B. *RESULTS OF VERIFICATION AND COMPARISON*

To validate the accuracy of the formulae presented in this paper, a comparative analysis was conducted between this paper, previous research, and FEA. Yura's formula [1], depicted in Eq. (31), is applicable for the approximate calculation of LTB strength where bracings are positioned on the compression flange. For the FEA, the LTBeamN [19-21] software was employed, utilizing a beam element modeling

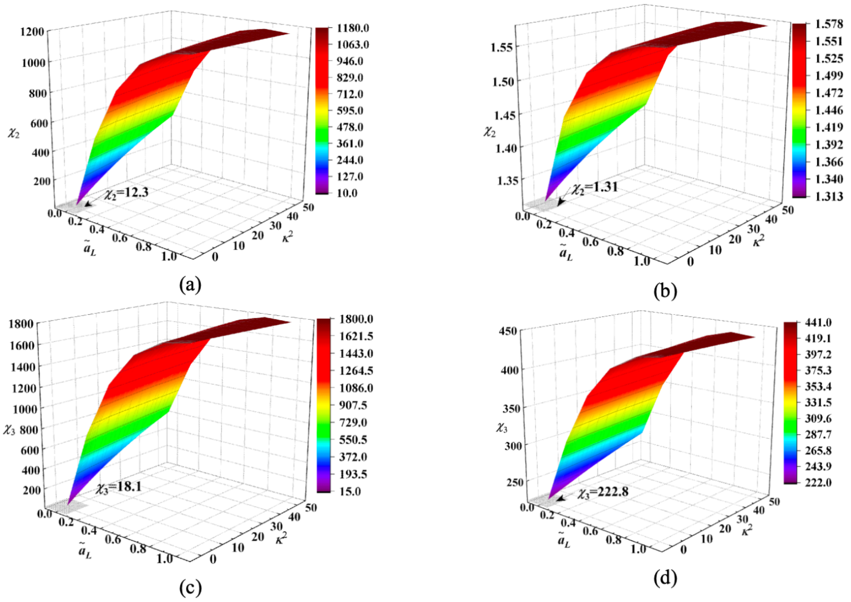

FIGURE 3. The value of χ_j for $n_b = 10$: (a) when $i = 1$, the value of χ_2; (b) when $i = 10$, the value of χ_2; (c) when $i = 1$, the value of χ_3; (d) when $i = 10$, the value of χ_3

TABLE 4. The calculation result for $i = 1$

h_0 (mm)	t_w (mm)	b_f (mm)	t_f (mm)	r (mm)
398.78	6.35	139.7	8.763	0

approach. The boundary conditions were configured as a simply supported beam with "cross-bracing," and the load consisted of equal end moments. Figure 4 illustrates the details, while Table 4 outlines the sectional parameters of the beam used in the example. The beam spans 40 ft (12192 mm) in length and features three lateral point bracings arranged at regular intervals.

$$M_{cr} = \sqrt{\left(M_0^2 + \frac{P_0^2 h^2 A}{4}\right)(1 + A)},$$
$$A = \frac{L^2}{\pi}\sqrt{\frac{0.67 n_b \beta_L}{E I_y L}}. \tag{31}$$

Figure 5 presents a comparative analysis of the calculation results derived from the formula proposed in this study, Yuar's formula, and the FEM, specifically when the lateral bracing is located at the compression flange ($\widetilde{a}_L = 1$). Additionally, Table 5 provides the LTB strength across various brace stiffness conditions. As evidenced by Table 5 and Figure 5, when the lateral point bracing is located at the compression flange, the formula proposed in this study exhibits excellent agreement with the FEM results, with a relative error margin not exceeding 1%, thereby demonstrating greater precision compared to Yura's formula.

To provide a clearer illustration of the error associated with the simple harmonic wave analysis (where the number of terms is taken as $n_b + 1$), a comparative analysis is presented in Figure 6. Notably, substantial discrepancies are evident in the computational outcomes. When $\widetilde{M}_{cr,(n_b+1)}$ equals $\widetilde{M}_{cr,n_b}$, the stiffness determined corresponds to the threshold stiffness of the lateral bracings. It is evident that the precision of this threshold stiffness is intrinsically linked to the accuracy of $\widetilde{M}_{cr,n_b}$ calculation. Employing the simple harmonic wave as the displacement function tends to underestimate the threshold stiffness value. Conversely, utilizing the simplified formula (Eq. (30)) introduced in this study yields a more precise value for $\widetilde{M}_{cr,n_b}$, resulting in a more accurate determination of the threshold stiffness.

TABLE 5. Comparison of LTB strength under varying brace stiffness conditions (Unit: $\times 10^3$ kN·m)

Brace stiffness β_L (kN/m)	$\widetilde{\beta}_L$	LTB strength of FEM	LTB strength of this study	Error 1	LTB strength of Yura	Error 2
0	0	22.88	22.88	–	22.88	–
19.90	0.070	64.17	64.32	0.23%	58.68	-8.55%
49.75	0.174	82.97	83.12	0.18%	77.94	-6.06%
100.81	0.353	107.22	107.47	0.24%	99.78	-6.94%
153.38	0.536	131.39	131.82	0.33%	116.78	-11.12%
190.07	0.693	151.25	151.95	0.46%	128.99	-14.71%
251.66	0.880	160.21	160.45	0.15%	141.91	-11.42%
353.06	1.235	174.16	174.55	0.22%	162.98	-6.42%
484.00	1.693	188.13	188.64	0.27%	186.04	-1.11%
489.87	1.713	188.64	188.64	0.27%	187.00	-0.87%
500.04	1.749	188.64	188.64	–	188.64	–

Note: Error 1 = [This study – FEM]/FEM; Error 2 = [Yura – FEM]/FEM.

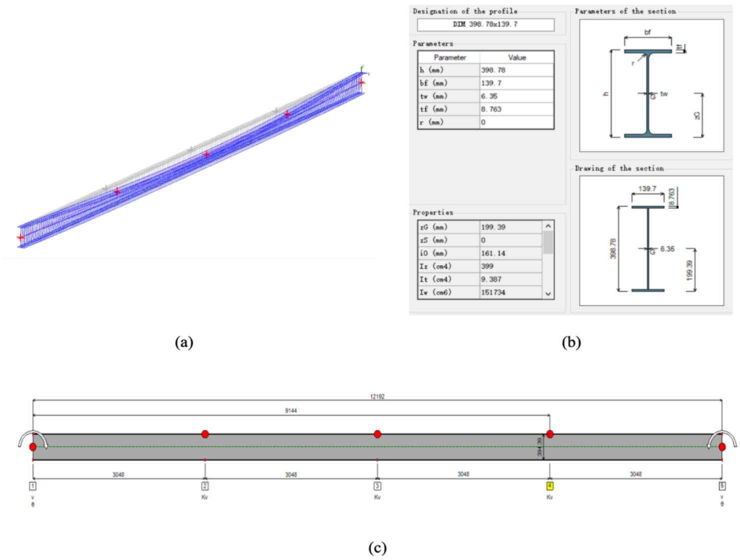

FIGURE 4. FEA parameters (Units: mm): (a)finite element analysis models; (b) section parameters; (c) brace positions

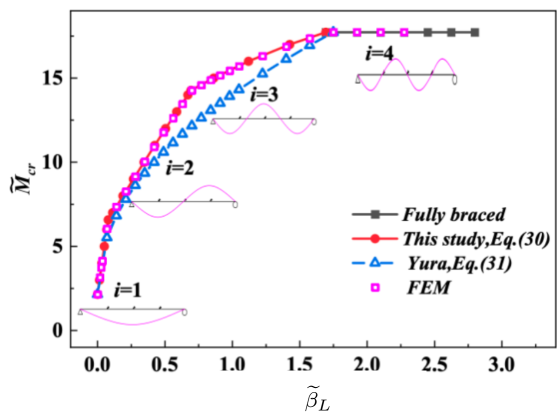

FIGURE 5. Comparison of LTB strength

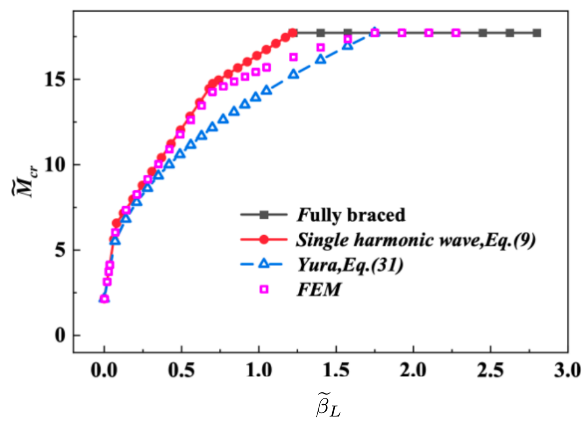

FIGURE 6. Comparison of single harmonic wave analysis, FEM, and Yura's formula

VI. CONCLUSION

In conclusion, this research delves into the derivation and analysis of LTB strength for I-beams with lateral bracings, employing both simple harmonic waves and Fourier series based on trigonometric functions as displacement functions. It underscores the significance of the number of terms in the displacement function for accurately calculating both the critical moment and the threshold stiffness, and offers reasonable suggestions for selecting an appropriate number of terms. The findings indicate that, when the beam is "fully braced" (meaning the brace stiffness is sufficient to allow buckling between the braces of the beam), the derived LTB strength expressions coincide, irrespective of whether a simple harmonic wave or Fourier series is adopted as the displacement function. Divergences in LTB strength formulas emerge solely in scenarios of "partially braced," where the brace is inadequate to permit buckling between braces. The optimal number of terms is intrinsically linked to the number of brace; hence, this study recommends setting the number of terms in the displacement function to when employing the energy method to ascertain the LTB strength of laterally braced beams.

The outcomes of this research present a novel perspective that is both straightforward and precise in addressing this type of problem. Despite inherent constraints in parameter selection and data handling, the conclusions drawn possess a high degree of reliability and practical relevance. It is worth noting that, while this study focuses solely on the influence of the number of terms, it does not delve into the influence of brace height. Consequently, future research endeavors should aim to further explore the influence of brace height on critical moment and threshold stiffness.

ACKNOWLEDGMENT

This work was supported by Scientific and Technological Innovation Programs of Higher Education Institutions in Shanxi(grant no. 2024L431), supported by Fundamental Research Program of Shanxi Province(grant no. 202503021212283), supported by Science and Technology Plan Project of the Department of Housing and Urban-Rural Development of Shanxi Province(grant no. JJKJ2025016), supported by Shanxi Vocational University of Engineering Science and Technology Research Fund Project(grant no.KJ202516) and Contracted Research Project(grant no.2025HX05008).

REFERENCES

[1] J. Yura, et al., "Bracing of Steel Beams in Bridges," Rep. No. 1239-4F, 1992.
[2] AISC, Specification for Structural Steel Buildings. Chicago: AISC, 2016.
[3] C. T. Nguyen, J. Moon, and H.-E. Lee, "Lateral–torsional buckling of I-girders with discrete torsional bracings," Journal of Constructional Steel Research, vol. 66, no. 2, pp. 170-177, 2010, doi: 10.1016/j.jcsr.2009.09.011.
[4] Y. Quanzhou, et al., "Precision Improved Local Buckling Analysis of Elastically Restrained Orthotropic Plates," Chinese Quarterly of Mechanics, vol. 35, no. 2, pp. 180-188, 2014.
[5] S. Amara, D. E. Kerdal, and J. P. Jaspart, "Effect of End Connection Restraints on the Stability of Steel Beams in Bending," Advanced Steel Construction, vol. 4, no. 3, pp. 243-259, 2008.
[6] D. Liu and R. Magliola, "End Forces on Crossframes in Horizontally Curved Steel I-Girder Bridges," Practice Periodical on Structural Design and Construction, vol. 15, no. 1, pp. 21-26, 2010, doi: 10.1061/(ASCE)SC.1943-5576.0000018.
[7] B. Siyuan, W. Jiali, and S. Feng, "An Analytical Beam-segment Superposition Method for Free Vibration of Braced Stepped Beams," Journal of Dynamics and Control, vol. 21, no. 3, pp. 85-95, 2023.
[8] B. Siyuan and Z. Jing, "Vibrational characteristics of a multi-span beam with elastic transverse supports of different shaped sections," Chinese Journal of Ship Research, vol. 15, no. 1, pp. 162-169, 2020.
[9] L. Dazhong and Z. Baoting, "Fourier Series Based on the Deflection Equation Expansion of Simple Beam," Transactions of Beijing Institute of Technology, no. 1, pp. 1-5, 2010.
[10] Z. Haijun, et al., "Transverse Vibration Analysis of Shafting Based on an Improved Fourier Series Method," Noise and Vibration Control, vol. 31, no. 4, pp. 68-72, 2011.
[11] Z. Wenfu, et al., "Infinite Series Solution and FEM Verification of Lateral-torsional Buckling of A T-section Cantilever Column Under Its Own Weight," Journal of Anhui Jianzhu University, no. 004, pp. 21-26, 2022.
[12] T. Genshu and Z. Lei, "A controversy and its settlement in the calculation of buckling moments of Thin-walled beams with monosymmetrical I-sections under distributed loads," Journal of Building Structures, vol. 23, no. 3, pp. 44-51, 2002.
[13] L. V. Liewu and S. S. Shen Zuyan, Stability of Steel Structural Members. Beijing, China: China Architecture & Building Press, 1983.
[14] N. S. Trahair, et al., The Behaviour and Design of Steel Structures to EC3. CRC Press, 2017.
[15] L. Zhan-ke, Z. Xu-hong, and H. Zi-qi, "An analysis on rationalization of total potential energy equation of steel members with flexural-torsional buckling," Engineering Mechanics, vol. 30, no. 3, pp. 82-88, 2013.
[16] X. Zhou, et al., "Study on general formula of critical moment of steel beam with flexural-torsional buckling," Journal of Building Structures, 2013.
[17] L. Zhan-ke and Z. Xu-hong, "General summation formulae of monosymmetry section constants of thin-walled members," Engineering Mechanics, vol. 34, no. 5, pp. 23-29, 2017.
[18] G. Winter, "Lateral Bracing of Columns and Beams," Journal of the Structural Division, vol. 84, no. 2, pp. 1561-1–1561-22, 1958, doi: 10.1061/JSDEAG.0000212.
[19] R. Piotrowski and M. Siedlecka, "Point Protection of Primary Beams of Steel Grillages Against Lateral Torsional Buckling," Advances in Science and Technology Research Journal, vol. 14, pp. 1-8, 2020, doi: 10.12913/22998624/121532.
[20] R. Piotrowski and A. Szychowski, "Impact of support closed section ribs on the critical moment for lateral torsional buckling of steel beams," Structure and Environment, vol. 10, 2018, doi: 10.30540/sae-2018-001.
[21] R. Piotrowski and A. Szychowski, "Lateral Torsional Buckling of Steel Beams Elastically Restrained at the Support Nodes," Applied Sciences, vol. 9, no. 9, p. 1944, 2019, doi: 10.3390/app9091944.